

# THE SAN JUAN FAULT: AN EAST-WEST TRENDING LEFT-LATERAL STRIKE SLIP FAULT INFERRED FROM ANALYSIS OF KINEMATIC INDICATORS, VANCOUVER ISLAND, BC

NOLAN LESCALLEET, Union College

Research Advisor: Dr. Matthew Manon

## ABSTRACT

We present data on the kinematics and geometry of a western segment of the San Juan Fault (SJF), which strikes sub-east-west near the southeastern tip of Vancouver Island, British Columbia, Canada. This fault delineates the boundary between metamorphosed volcanic and plutonic rocks of the Wrangellia terrane, specifically West Coast Crystalline island intrusions, to the north from the Pandora Peak unit and Leech River Complex of the Pacific Rim terrane to the south. Detailed geologic mapping of the study area suggests the San Juan Fault is not a discrete fault, but rather a complex fault zone. The SJF is conjectured to be a left-lateral slip based on its observed, high-angle dip through LITHOPROBE studies, and the eastward displacement of West Coast Crystalline rocks, yet kinematic support is lacking. We present fault kinematic indicators from six locations, including a total of 203 slickenlines and shear-sense fractures that suggest left-lateral slip with a component of oblique thrust motion. Secondary faults predominantly trend northeast-southwest or northwest-southeast and show evidence for both sinistral and dextral slip. These secondary faults likely formed in response to continued accretion of the later Pacific Rim and Crescent terranes, and continued subduction of the Juan de Fuca plate under Vancouver island, leading to increased strain on the transpressional strike-slip system. The San Juan fault branches and splay towards its western extent, which may be due to increased northeast-directed strain. Thus, the San Juan fault is an east-west trending, left-lateral high angle strike-slip fault with an oblique thrust component.

## INTRODUCTION

The Cascadia subduction zone is defined by the Juan de Fuca plate that continues to creep eastward under the North American plate at a rate of  $\sim 40$  mm/yr (Demets et al., 1990). This active margin has

progressed Vancouver Island's deformation, shaping the landscape with mountainous topography and a complex fault system (Project Director's Fig. 1). The San Juan Fault (SJF) is a sub-east west trending fault transecting through the southeastern uplands of Vancouver Island, just north of Port San Juan and west of the Cowichan Valley. It is associated with the southwestern regional faulting of the island including the Leech River Fault, Port Renfrew Fault, Survey Mountain Fault, the West Coast Fault, and the Tofino Fault. The Leech River Fault and Port Renfrew Fault are low-angle, northeast-dipping, oblique-thrust faults with left-lateral motion lying just south of the SJF (Clowes et al, 1986). The Port Renfrew Fault splays  $30^\circ$  to the south of the SJF (Muller, 1976; Rusmore and Cowan, 1984). The SJF has been interpreted in the literature to be a high-angle left-lateral fault with a minor thrust component (Rusmore and Cowan, 1984; England and Calon, 2002; Johnston and Acton, 2003), however evidence is lacking on the kinematics and geometry of the San Juan Fault (Project Director's Fig. 2).

Our objectives in this paper are to interpret macroscopic brittle deformation to understand the kinematics of the westernmost San Juan Fault. We focus on analyzing the following kinematic indicators: (1) slickenlines, a form of fault striae that result from the abrasion of two fault rocks sliding against one another in the direction of fault slip, and (2) slickenside-surface Riedel shears, which are resultant subsurface fractures angling away from the fault surface in the direction of shear. We will also utilize fieldwork and aerial photography correlated at different outcrops to estimate the size of the SJFZ.

## METHODS

### Field Collection

A total of six excavated roadcut and/or quarry localities adjacent to a western segment of the San Juan fault were chosen based on each outcrop's abundance of smooth, polished surfaces, or fault surfaces. These localities are herein named: (1) Igloo Quarry (IQ), (2) Adjacent Splay Quarry (ASQ), (3) Shortcut Road West (SRW), (4) Shortcut Road East (SRE), (5) Pandora Peak Main Road West (PPMRW), and (6) Pandora Peak Main Road East (Fig. 1). Note, Pandora Peak Main Road and Shortcut Road localities are abandoned logging roads that have each been divided into east and west outcrops based on differing rock type and location.

We used slip-sense orientations on fault planes and corresponding secondary structures to interpret fault kinematics. We focused on recording the orientations of slickenside fault surfaces, which preserve a fault's slip history through slickenlines (Petit, 1987; Almendinger, 1989). We followed Petit (1987) in the utilization of two main slickenside shear-sense indicators: localized recrystallization of minerals and surface Riedel shears. Crystallization of minerals (i.e. quartz and calcite) occur on the relative leeward face of surface asperities in congruous steps in the direction of fault shear (Petit, 1987). Riedel shears are described as shallow fractures dipping away from the fault plane in the direction of slip sense. It is characteristic for these fractures to become recrystallized with quartz and calcite (Petit, 1987).

Four oriented samples were taken from IQ (SJ16NL02 and SJ16NL03), ASQ (SJ167NL01), and SCR (SJ16NL04) and a non-oriented sample was taken from PPMRE (SJ16NL05) and cut into thin sections to look for subsurface kinematic fractures and geologic unit identification. Thin sections were cut, carbon-coated, and analyzed at Union College utilizing a scanning electron microscope (SEM) and back scatter detector (BSD) to identify different mineral assemblages for lithologic identification.

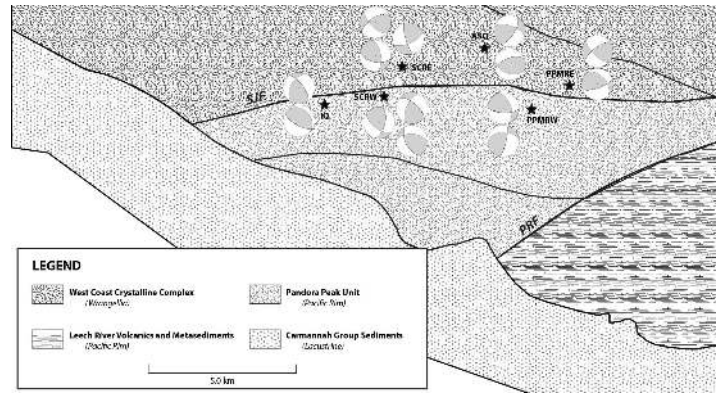


Figure 1. Geologic map of the study area with GPS referenced localities. Focal mechanisms from the dominant fault sets are pinned to each outcrop (After Rusmore and Cowan (1984) and Massey et al., 2005).

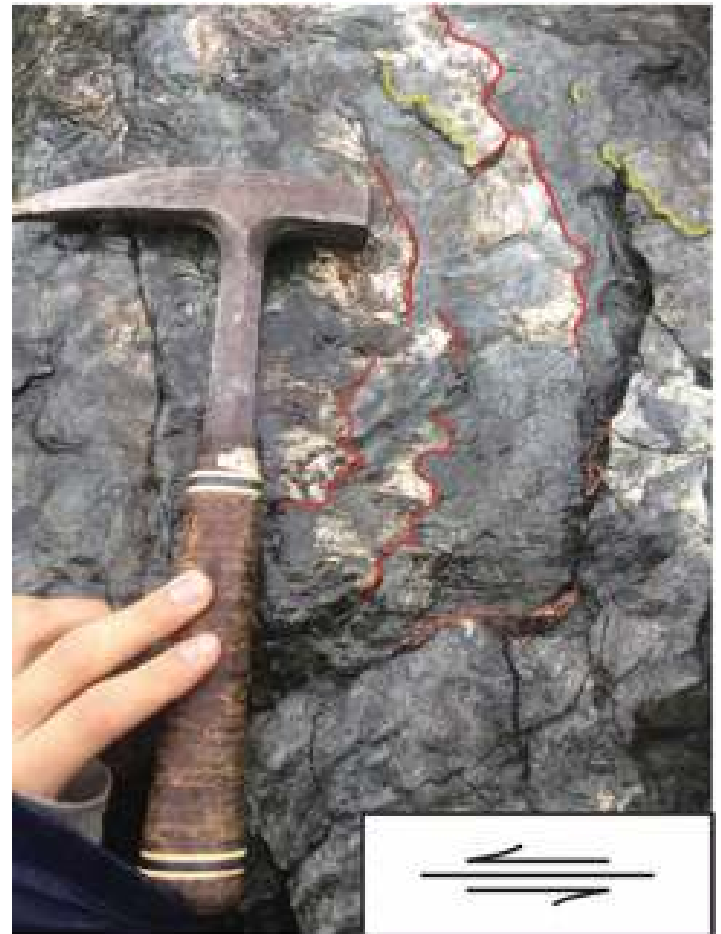


Figure 2. Field image of slickenside surface depicting both utilized shear-structures: (1) congruous-crystallization steps (red), and (2) Riedel shears (yellow). Bottom right illustration provides schematic of right-lateral (dextral) slip as indicated by the shear-sense structures.

## Data Analysis

After field data acquisition, fault populations were plotted using Faultkin and Stereonet3D computer programs (Marrett and Allmendinger, 1990; Allmendinger, 2012). As the data show multiple orientations of shear and therefore fault planes, we divided our data by locality and further sub-grouped the dominant fault plane orientations (Allmendinger, 1989). It is common for slickenline orientations to vary between 10-20 degrees on the same fault plane. In the field, we measured slickenlines across all outcrop surfaces to get a representative spatial distribution of the dominant slip-sense in the region. (s).

## RESULTS

We isolated the results of individual outcrops due to (1) different geologic units having different structural histories, and (2) the likely potential for differences in strain experienced across the study area. Here, we provide brief descriptions of each locality followed by correlating spatial trends in geometries and kinematics of dominant fault plane orientations.

### Locality Description

*The Igloo Quarry (IQ)* is the westernmost outcrop observed (Fig. 3). It is a massive bedrock quarry that opens to the southeast and consists of unfossiliferous, green-, blue-, gray-weathered volcanics with small, discontinuous, ductile-green intrusions. SEM and BSD analysis indicate its mineral assemblage coincides with fine-grained greywackes of the Pandora Peak unit. The green intrusions are composed of epidote and chlorite composing the green tuff of this unit (Rusmore and Cowan, 1984). Neither apparent bedding or foliation were observed in the field or under thin section.

*The Adjacent Splay Quarry (ASQ)* provides the northernmost extent of the study area (Fig. 3). It is a partially water-infilled quarry with well-polished, green-, black-, tan-weathered salt-and-pepper gneisses with no distinct bedding. Mineral assemblage is dominated by plagioclases, pyroxenes, and chlorites with apatite and ilmenite accessory minerals, likely of the West Coast Crystalline Complex (Fairchild and Cowan, 1982).

*Pandora Peak Main Road* is a ~2.0-km abandoned logging road that we split into two localities – Pandora Peak Main Road East (PPMRE) and Pandora Peak Main Road West (PPMRW) (Fig. 3). PPMRE trends to the northeast and contains a similar mineral composition as ASQ; therefore, rocks are inferred West Coast Crystalline island intrusions (Fairchild and Cowan, 1982). Alternatively, PPMRW contains fine-grained, blue-, gray weathered rocks. Rocks appear

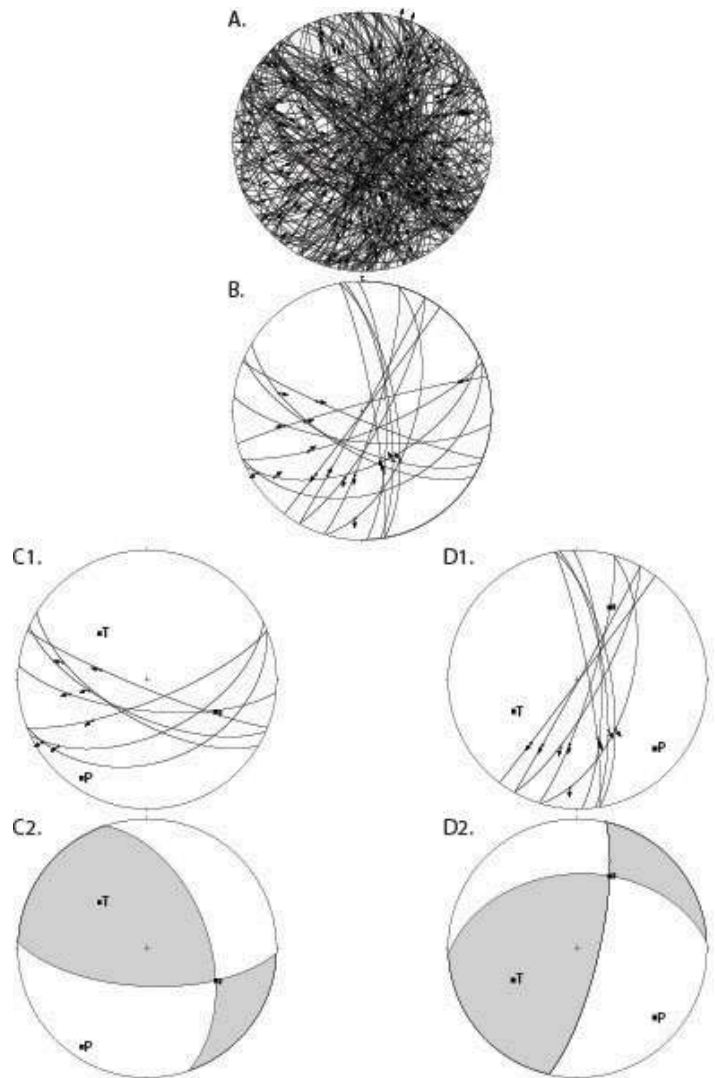


Figure 3. Example of methodology in grouping fault plane orientations from data taken at PPMRW. (A) Fault plane and slick data from all observed localities plotted on one stereograph. (B) Stereograph depicting slip data from PPMRW. (C1) The primary fault geometry with corresponding slicks of PPMRW; best fit plane strikes  $92.5^{\circ}$  E and dips  $65.8^{\circ}$  S. (C2) Focal mechanism of plotted data from (C1). The trend and plunge of the P- and T-axes are  $213.2^{\circ} - 15.8$  and  $323.6^{\circ} - 51.0^{\circ}$ , respectively. (D1) Secondary fault orientation of PPMRW; strike and dip are  $12.7^{\circ}$  and  $76.3^{\circ}$  of the best fit fault plane. (D2) Focal mechanism of (D1) fault set. Trend and plunge of the P- and T-axes are  $243.4^{\circ} - 43.8^{\circ}$  and  $132.0^{\circ} - 20.9^{\circ}$ .

**Table 1.** Fault plane solutions and corresponding measurements of slicks categorized by the strikes of dominant fault orientations

Location	Strike	Dip	Trend	Plunge	Rake (Aki-Richards)	Slip
<i>West-Southwest Striking</i>						
PPMRE <sub>1</sub>	232.8	71.3	44.2	23.8	25.2	TL
SCRE <sub>1</sub>	238	65.6	45.3	25.9	28.7	TL
ASQ <sub>1</sub>	249.1	57.4	22.8	48.4	62.7	TL
<i>East Striking</i>						
PPMRW <sub>1</sub>	92.5	65.8	250.9	39.3	44	TL
PPMRE <sub>2</sub>	70.1	69.5	226.6	46.7	51	TL
SCRE <sub>2</sub>	100.5	56.9	265.9	21.2	33.7	TL
IQ <sub>1</sub>	119.2	66.1	226.5	65.1	82.8	TL
<i>North-Northeast Striking</i>						
ASQ <sub>2</sub>	32.7	65.2	198.8	27.5	30.5	TL
PPMRW <sub>2</sub>	12.7	76.3	177	47.8	49.7	TL
SCRW <sub>1</sub>	14.1	59.4	35.8	32	142	TR
<i>Southeast Striking</i>						
SCRE <sub>3</sub>	163.2	76.5	22.9	24.2	25	TL
SCRW <sub>2</sub>	153.9	56.4	182.9	36.1	134.9	TR
<i>Northwest Striking</i>						
IQ <sub>2</sub>	322.6	67.8	119.6	43.7	48.3	TL
SCRW <sub>3</sub>	309.9	64.2	115	28	31.5	TL

to be the same greywackes seen at IQ, however no samples were taken for further analysis.

*Shortcut Road* is a ~2.5-km abandoned logging road that was also spatially segmented into Shortcut Main Road East (SCRE) and Shortcut Main Road West (SCRE) (Fig. 3). No sample was taken from SCRW, yet rocks have similar lithologic field descriptions as Pandora Peak greywackes. A sample from SCRE indicates rocks are of the West Coast Crystalline unit.

### Spatial Trends

We used spatial trends of the compiled fault geometries surrounding the SJF to discern probable regional slip along the large fault system. As can be seen by Fig. 3, at least two fault orientations were produced from each locality with differing kinematics. The observed fault set geometries have several orientations, yet twelve of the fourteen identified orientations are dominated by high angle faults depicting left-lateral slip-sense (Table 1).

### Left-Lateral

West and southwest striking fault orientations are observed at PPMRE, SCRE, and ASQ. These faults dip to the north at high angles of 71.3°, 65.6°, and 57.4°. The high dip angle is immediately indicative of either strike-slip or oblique movement (Biddle and Blick, 1985). Relative hanging wall motion at PPMRE and SCRE recorded by slicks indicates rakes of 25.2° and 28.7°. These shallow slip angles support a sinistral

horizontal movement along the slickenside. The slip calculated at ASQ was 62.7°, also supporting left-slip coupled with a thrusting dip-slip component.

Four fault sets at PPMRW, PPMRE, SCRE, and IQ were observed having relative east strikes. All fault sets have high angle geometries dipping to the south at 65.8°, 69.5°, 56.9, and 66.1°, and preserve oblique left-slip motion along the fault.

Three localities abutting the mapped SJF – at ASQ, PPMRW, and SCRW – record a secondary fault orientation striking to the north or north-northeast with high dip angles. A sub-southeast striking fault set observed at and SCRE records sinistral movement and splays at ~60° from the west-southwest-trending SJF. Northwest-striking, left-slip fault sets were seen at IQ and SCRW.

### Evidence for minor Right-Lateral kinematics

The final two fault sets were observed at SCRW and display sinistral movement: one east and one southwest dipping fault sets. These indicate shallow, thrust-right dip-slip kinematics.

### DISCUSSION

Here we correlate the dominant fault orientations seen at all outcrops and interpret their regional implications towards the structural history of Vancouver Island.

### Left-lateral Interpretations

Southwest striking (fault data taken from PPMRE, SCRE, and ASQ strikes 239.97° (± 9.13) and dips 64.77° (± 7.37°) to the northwest. We interpret this fault set to be the representative fault data on several grounds: (1) it corresponds with previous seismic mapping of the SJF, (2) the reoccurrence of this fault set across a spatial distribution of ~8.10-km<sup>2</sup>, and (3) it corresponds with previous inferences of left-slip motion associated with displaced West Coast Crystalline rocks north of the Pacific Rim terrane and delineated by the SJF (Rusmore and Cowan, 1984; Clowes et al., 1986; England and Calon, 2002; Johnston and Acton, 2003).

The east-striking fault sets at PPMRE, PPMRW, SCRE, and IQ, oriented 95.58° (± 25.48°), indicate

an interesting phenomenon. They record a relative left-slip oblique thrusting motion with an increasing clockwise rotation along an east-to-west transect, that is, the easternmost set at PPMRE is striking  $70.1^\circ$  with a rake of  $51^\circ$ , while the orientation at IQ strikes  $119.2^\circ$  and thrusts  $82.8^\circ$ . These observations indicate a rotation of strike by  $30.1^\circ$  and a counterclockwise rotation in dip-slip of  $31.8^\circ$ . One interpretation of these data is that they are recording an east-to-west gradient of synthetic shearing along the SJF, which could be due to continued subduction of the Juan de Fuca and collision of the Crescent terrane (Johnston and Acton, 2003). An alternative interpretation would describe this fault set recording antithetic shearing of the SJF as the set does not change strike by more than  $\sim 60^\circ$  relative to the sub-west trending SJF, which follows Riedel shear modeling, yet we would expect to see dextral slip (Biddle and Blick, 1985; Kim and Anderson, 2006).

ASQ and PPMRW spatially depict north and northeast trending sinistral movement over a  $\sim 2.66$ -km transect at  $\sim 45^\circ$ - $60^\circ$  to the SJF. These data likely represent high angle synthetic faults following transpressional Riedel shearing models, which are characteristic of strike-slip systems (Rao, 2011). We would additionally expect to see this as our study area represents the western tip of the SJF, representing the process zone that often has secondary splays descending from strike in the direction of shear (Kim and Sanderson, 2006).

The northeast and southwest dipping fault sets are interpreted as a separate system to the SJF and alternatively preserve the continued under-thrusting of the Juan de Fuca plate. Thus, the northeast dipping faults on the western extent at SCRW and IQ are probable synthetic thrust faults and the southwest dipping fault at SCRE is a probable antithetic thrust fault.

### Right-lateral Kinematics

Two dextral faults are identified at SCRW, but are interpreted to be from different strains. One set trends  $14.1^\circ$ - $194.1^\circ$  to the southwest, making it splay  $\sim 45^\circ$  from the SJF. Thus, this set is interpreted as a conjugate, antithetic fault off the sinistral-shearing SJF (Rao, 2011). The second fault orientation dips to the northeast at  $56.4^\circ$ , and is either an alternative antithetic

fault from Juan de Fuca plate under-thrusting, or is attributed to the bending and block rotation model proposed by Johnston and Acton (2003), which is further discussed below.

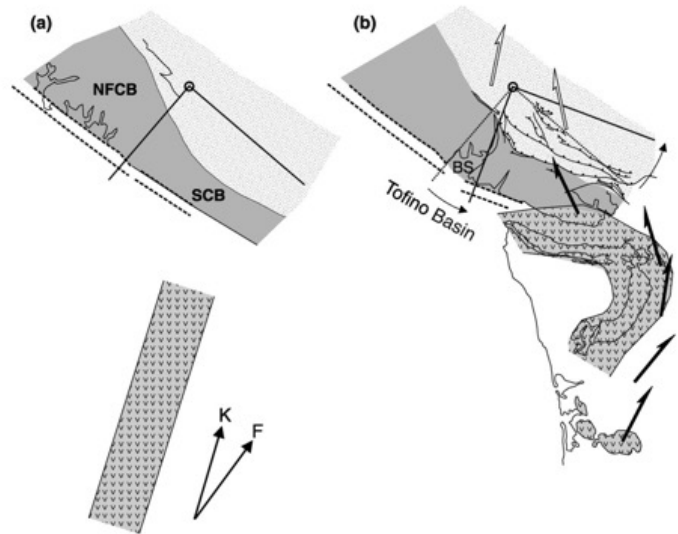


Figure 4. Schematic interpretation of the formation of the Vancouver Island and Olympic oroclines as a result of the Pacific Rim (K) and Crescent (F) terranes colliding with Vancouver Island (Johnston and Acton, 2003). (A-B) Vancouver Island prior and post collision of terranes. NFCB (North Fixed Crustal Block) remained stationary while the SCB (Southern Crustal Block) was rotated by  $20^\circ$  due to the amalgamations, resulting in the formation of the Cowichan fold and thrust belt, northeast of our study area, and the extensional Tofino Basin, offshore of Vancouver Island. Johnston and Acton (2003) also postulate that this collision may be responsible for sinistral shearing seen near our study area.

### Regional Implications

Faulting surrounding the San Juan fault system is complicated with varied fault geometries displaying both sinistral and dextral motions. the simplest model describes a single high-angle thrust fault dipping to the northeast resulting from the collision of the Crescent terranes, like faulting of the Cowichan fold and thrust belt to the northeast (Johnston and Acton, 2003). This is not the scenario we observe. however. We instead observe a high-angle sinistral fault zone trending  $239.97^\circ (\pm 9.13)$  to the southwest with an oblique thrust component. As proposed by Johnston and Acton (2003), the SJFZ is interpreted to be formed at the same time as the formation of the Southern Vancouver Island Orocline (SVIO). These authors suggest by  $20^\circ$  of counterclockwise bending of Vancouver Island

has occurred relative to stable North America since the Eocene (Fig. 4) due to post-Late Cretaceous amalgamation of the later Pacific Rim and Crescent terrane (Johnston and Acton, 2003). Johnston and Acton (2002) hypothesize resultant northeast trending sinistral faults and northwest trending dextral faults to accommodate the concluded block rotation (Johnston and Acton, 2003). Our results agree with this model.

## CONCLUSIONS

Faulting in southwestern Vancouver Island is defined by medium-high angle thrusting due to the amalgamation of the Pacific Rim and Crescent terranes underthrusting Vancouver Island during the Late Cretaceous. Although kinematics of faulting surrounding the SJF are relatively known, movement has only been inferred. Our study provides the first detailed kinematic analysis of the SJF analyzing slickenlines and surface Riedel shears along mesoscale faults on the fault's westernmost extent. The data shows a sub-vertical fault system at least 750-meters wide that is dominated by oblique left-slip movement with minor northwest striking dextral shearing. Our findings support the bending and southern Vancouver Island block rotation model and the development of the Southern Vancouver Island Orocline. We suggest that future studies should look at (1) correlating our slickenside kinematic indicators with microstructural brittle deformation and macroscale and microscale ductile kinematics, and (2) observing kinematics of major fault splays (i.e. Port Renfrew Fault and the San Juan Fault Splay) to better understand the regional deformation along the San Juan Fault Zone.

## REFERENCES

- Allmendinger, R. W., Cardozo, N., & Fisher, D. M. (2011). *Structural geology algorithms: Vectors and tensors*. Cambridge University Press.
- Allmendinger, R. W., Gephart, J. W., & Marrett, R. A. (1989). Notes on fault slip analysis. *Geol. Soc. Am. Short Course*, 66.
- Biddle, K. T., & Christie-Blick, N. (1985). Glossary—strike-slip deformation, basin formation, and sedimentation.
- de Jossineau, G., Mutlu, O., Aydin, A., & Pollard, D. D. (2007). Characterization of strike-slip fault–splay relationships in sandstone. *Journal of Structural Geology*, 29(11), 1831-1842.
- DeMets, C., Gordon, R. G., Argus, D. F., & Stein, S. (1990). Current plate motions. *Geophysical journal international*, 101(2), 425-478.
- England, T. D. J., & Calon, T. J. (1991). The Cowichan fold and thrust system, Vancouver Island, southwestern British Columbia. *Geological Society of America Bulletin*, 103(3), 336-362.
- Fairchild, L. H., & Cowan, D. S. (1982). Structure, petrology, and tectonic history of the Leech River complex northwest of Victoria, Vancouver Island. *Canadian Journal of Earth Sciences*, 19(9), 1817-1835.
- Kim, Y. S., & Sanderson, D. J. (2006). Structural similarity and variety at the tips in a wide range of strike-slip faults: a review. *Terra Nova*, 18(5), 330-344.
- Marrett, R., & Allmendinger, R. W. (1990). Kinematic analysis of fault-slip data. *Journal of structural geology*, 12(8), 973-986.
- Massey, N. W. D., D. MacIntyre, P. Desjardins, and R. Cooney (2005), *Digital geology map of British Columbia*, BC Ministry of Energy and Mines Geological Survey Branch.
- Muller, J. E. (1977). Evolution of the Pacific Margin, Vancouver Island, and adjacent regions. *Canadian Journal of Earth Sciences*, 14(9), 2062-2085.
- Rao, G., Lin, A., Yan, B., Jia, D., Wu, X., & Ren, Z. (2011). Co-seismic Riedel shear structures produced by the 2010 M<sub>w</sub> 6.9 Yushu earthquake, central Tibetan Plateau, China. *Tectonophysics*, 507(1), 86-94.
- Rusmore, M. E., & Cowan, D. S. (1985). Jurassic–Cretaceous rock units along the southern edge of the Wrangellia terrane on Vancouver Island. *Canadian Journal of Earth Sciences*, 22(8), 1223-1232.
- Waldron, J. W. F., Barr, S. M., Park, A. F., White, C. E., & Hibbard, J. (2015). Late paleozoic strike-slip faults in maritime Canada and their role in the reconfiguration of the northern Appalachian orogen. *Tectonics*, 34(8), 1661-1684.

